

Antenna for a Cranial Implant: Simulation Issues and Design Strategies

Alberto Jose Moreno Montes¹, Ismael Vico Trivino¹, Marko Bosiljevac², Miroslav J. Veljovic¹, Zvonimir Sipus² and Anja K. Skrivervik¹

¹ Microwave and Antenna Laboratory, Ecole Polytechnique Fédérale de Lausanne, CH-1015 Lausanne, Switzerland
anja.skrivervik@epfl.ch, ismael.vicotrivino@epfl.ch, miroslav.veljovic@epfl.ch

² Faculty of Electrical Engineering and Computing, University of Zagreb, Croatia,
marko.bosiljevac@fer.hr, zvonimir.sipus@fer.hr

Abstract—The design of a specific antenna for a cranial implant is used to illustrate design and simulation issues linked to implantable antennas. After a brief introduction, we will review the requirements for the antenna, and go through the design process, discussing the tools used and the issues encountered. The final design will then be presented and discussed

Index Terms—antennas, electromagnetics, propagation, measurements

I. INTRODUCTION

The aim of this contribution is to present and discuss certain aspects of the design process of an implantable antenna, illustrated by a practical case, a cranial implant.

Before starting the design of an antenna for a communication link, the system or design engineer usually first checks the feasibility of reaching the antenna requirements (gain, bandwidth, efficiency) taking into account the system constraints (real space allotted to the antenna, frequency) using for this simple approximations and fundamental limits. Examples start from the classic formula linking the far field limit to the antenna size, over closed form formulas giving the radiation characteristics for radiating apertures assuming the field distribution (see for instance [1]) to limits on side lobe levels in antenna arrays. For the case of electrically small antennas, as is the case in this contribution, fundamental limits on performance versus electrical size have been studied since over 70 years (see for instance [2, 3] for an overview. For the case of implanted antennas, the community has just started studying the fundamental limits on performance, but interesting preliminary results are available [4-6]. Once this is checked, the design procedure starts, usually by reviewing the relevant literature and then by checking and optimizing interesting design candidates using an in-house or a commercial solver. The initial design (dipole, monopole, patch, PIFA, etc.) will be defined by the available space the latter's form factor.

In the case of wearable or implantable antennas, a model of the human body will be used in the design process. It

should be as simple as possible to shorten the simulation time, but obviously, it should also be accurate enough to enable reliable results. Such models range from very detailed and precise description of the human body (e.g [7]) to simple homogenous or multilayered canonical shapes, typically parallelepipeds, cylinders, spheres or a combination thereof.

The design case reported in this contribution concerns an antenna for an implant placed in the skull bone, which should communicate the data measured by a neuro-sensor to a transceiver placed a few millimeters above on the cranium, on a dielectric spacer. The frequency of operation should be 5.8 GHz, the space allotted to the antenna is of 10mm x 10mm x 2mm, and the transmission attenuation should be less than 50 DB over a bandwidth of 50 MHz to ensure the requested data rate of communication. In the following sections, we will first present some first analysis of performances using a canonical model [8]. The design process and strategies used will then be discussed, followed by issues concerning the simulations. Finally, results will be shown.

II. DESIGN REQUIREMENTS

The design requirements are as follows:

- Implanted node placed in the bone layer, either on top of the head or behind the ear.
- Wearable node placed close to the skin using spacer (material to be defined). The antenna for the wearable node will be a simple patch antenna.
- Dimensions for the implanted antenna, including biocompatible layer on top: 10x10x2 mm³.
- The biocompatible material to be used should be either PEEK ($\epsilon_r=3.2$, $\tan \delta=0.01$) or Zirconia ($\epsilon_r=29$, $\tan \delta=0.002$).
- Frequency of operation: 5.8GHz
- S₂₁ between nodes: better than -50dB in a bandwidth of 100 MHz.

Two positions of the implant are possible, either the top of the head or at behind the ear. The tissues and their thicknesses are given in Table 1.

TABLE I. HEAD MODEL

Location	Thickness	Skin	Fat	Muscle	Bone	CSF
Behind the ear	Min. (mm)	1.8	1	1.6	4.4	5
	Nom. (mm)	2.2	4.8	2.4	5	
	Max. (mm)	2.75	9.9	8	10.3	
Top of the head	Min. (mm)	1.5	1.5	0	5	5
	Nom. (mm)	1.7	3.1		6.2	
	Max. (mm)	2.8	8		8	

TABLE II. DIELECTRIC PROPERTIES OF HEAD TISSUES AT 5.8 GHz

Tissue name	Relative permittivity	Loss tangent
Cerebro Spinal Fluid (CSF)	60.47	0.40
Bone cortical	9.70	0.37
Muscle	48.48	0.32
Fat	9.90	0.26
Skin Dry	35.10	0.33

III. CANONICAL MODEL

In order to assess the attenuation due to the human head, we first analyze the canonical problem illustrated in Figure 1.

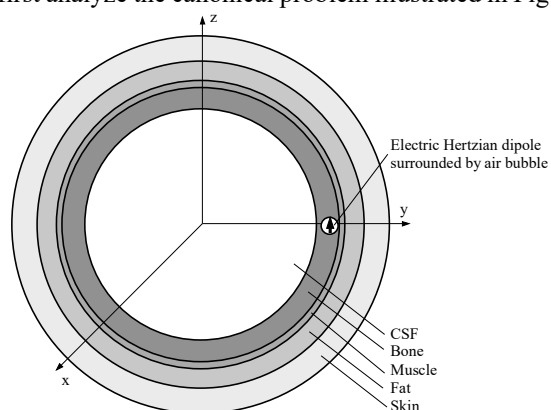


Fig. 1. Figure 1: Canonical problem of a Radiating source placed in a human head

We consider an overall radius of 10 cm, and the thicknesses of bone, muscle (when relevant), fat and skin are the nominal thicknesses given in Table 1. The dielectric properties of the tissues are shown in Table 2 [10]. The source is a Hertzian dipole oriented in parallel to the tissue interfaces, and placed in an air bubble having a radius (r_{impl}) of 1mm or 2 mm.

The power density normalized to the input power field along the y-axis is represented in Figure 2 for the behind the ear location (worst case). The decay is very strong close to the source, due to the near field losses [6]. These losses are weaker in the case of the larger lossless encapsulation, as expected.

We see that there are three contributions to the losses as the waves travels through the tissues: The losses due to the

near field, the losses due to the propagating field and the reflections. The antenna designer has no influence on the two latter. However, we also see that if the near field is confined in the lossless encapsulation around the antenna losses can be drastically reduced.

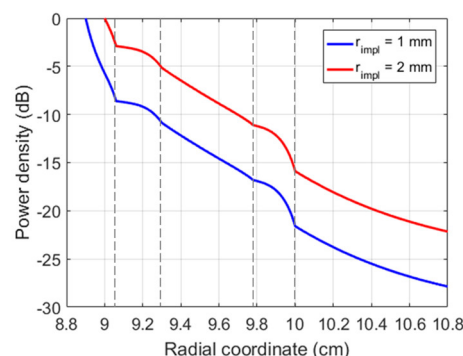


Fig. 2. Relative available power density as a function of distance for an elementary source placed behind the ear. Two different radius of the air encapsulation around the source are considered: 1mm and 2 mm. The limits of the bone, muscle fat and skin layers are indicated by dashed lines

In a design process, it is thus useful to be able to visualize the near field close to the antenna, using the data obtained by usual commercial or in-house simulation tools. Unfortunately, most of commercial solvers do not have this option in built. A way to overcome this issue is to build a post-processing tool allowing extracting the near field from the total field obtained from the numerical simulations [9]. To this aim, an estimation of the propagating contribution of the field is subtracted from the total field yielding an estimation of the near field. The estimation of the propagating contribution of the field is obtained by observing that in the far field, the field decreases with the inverse of the distance and the radial component of the field is equal to zero. In order

to check the procedure, the near field of a half wave dipole was estimated from the total field obtained by numerical simulations to the exact value. The comparison is shown in Figure 3:

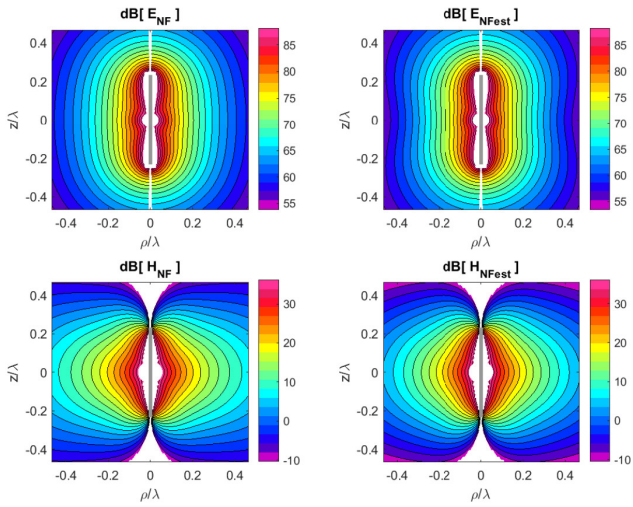


Fig. 3. Near field for the half-wave dipole oriented along z . Theoretical values on the left, estimations on the right.

IV. DESIGN PROCESS

The design process will be detailed for the location behind the ear, as this is the worst case due to the presence of the muscle layer above the antenna. The procedure is the same for the location on the top of the head.

For the design phase we select to us a simple model reprinting the human head: a parallelepiped having four or five layers: CSF, bone, muscle (if relevant to the position) fat and skin. A more detailed model can be used to check the validity of the design at the end of the latter. We use in the design phase the nominal thicknesses given in Table 1. The model is depicted in Figure 4.

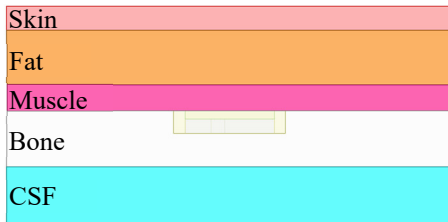


Fig. 4. Phantom used in the design phase

Due to the form factor of the volume given to the antenna, a printed antenna was selected for the initial design. The PIFA, having a smaller surface than a regular patch antenna and the potential for a better bandwidth is a good candidate for an initial design. The steps we followed for the design were the following:

1. Initial design in a lossless homogeneous medium, usually the medium which is in contact with the antenna, in our case muscle or fat (discarding the

losses). Neglecting the losses will give us a hint on the potential bandwidth of the antenna. In this step, we should keep the height of the PIFA as thin as possible while reaching a good enough bandwidth. Indeed, a thinner PIFA will allow for a thicker biocompatible superstrate, and thus less losses due to near fields.

2. Add losses in the medium and re-tune. This tuning is minimal.
3. Add encapsulation and re-tune. This step allow to assess the effect of this encapsulation, and select the best possible material. In this step the visualization of the near field can help.
4. Go to multilayered model, and re-tune.
5. Test for variations on model dimensions and on variations of the nominal thicknesses of the layers.
6. Add wearable antenna and study S_{21} for different spacer materials. Re-tune antennas if necessary.

We learned the following facts in the different steps:

1. In order to achieve small enough transverse dimensions to fit the specification, we had to use a substrate with a high dielectric permittivity for our PIFA. We selected a TMM10i substrate ($\epsilon_r=9.9$) with a thickness of 1.27mm. The latter was the selected as a good compromise, giving enough bandwidth but leaving 0.73mm for the encapsulation.
2. Adding the losses did of course enlarge the S_{11} bandwidth, but not the potential S_{21} bandwidth between the two nodes.
3. We had the choice between Zirconia and PEEK for the biocompatible superstrate. Zirconia, due to its high permittivity, lead to a non-negligible reduction in the dimension of the antenna, and thus of the bandwidth. Moreover, this reduction in size also lent to higher near fields, resulting in a 10dB smaller S_{21} between the implanted and wearables nodes for the Zirconia superstrate. We thus selected PEEK. Figure 5 shows the near field of the antenna with and without encapsulation.
4. The large difference of permittivity between the layers create a guiding effect reducing the radiation in the desired broadside direction. This effect is illustrated on Figure 6. To mitigate the losses due to this lateral guiding, we decided to place our PIFA into a cavity by metalizing the lateral walls of the dielectric substrate. In doing this, care should be taken to ensure that there are no resonance frequencies of the cavity inside the useful band of the antenna.
5. The lateral dimensions used (25mm x 23mm) proved to be large enough for or purpose. This was tested by comparing with larger phantoms. It is however crucial to properly terminate the lateral walls of the phantom by absorbing boundary conditions.

V. FINAL DESIGN

The antenna obtained using this design process is depicted in Figure 7, with the relevant dimensions in Table 3.

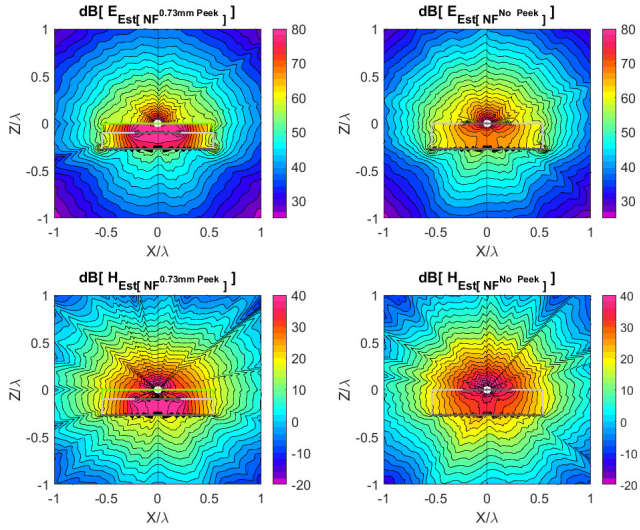


Fig. 5. Near field radiated by the PIFA in presence or absence of a PEEK superstrate (homogeneous phantom (muscle))

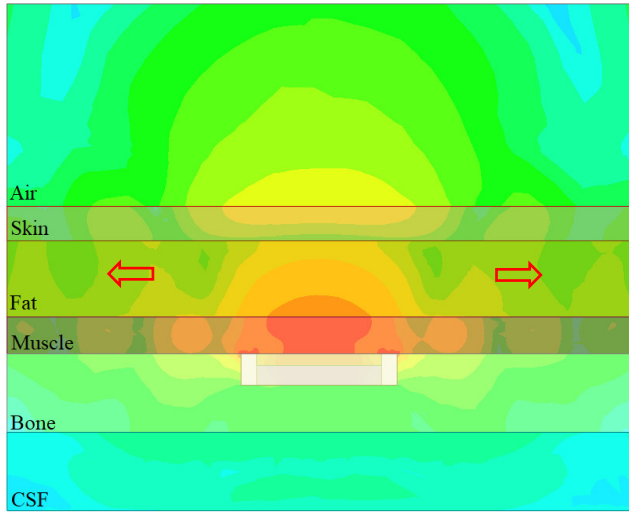
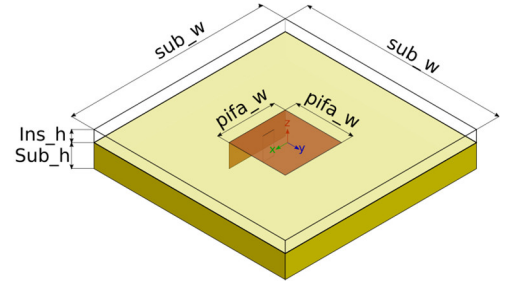
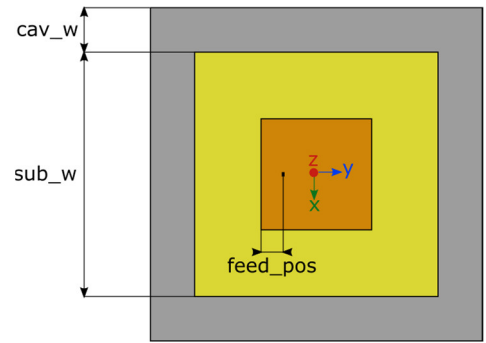


Fig. 6. E-Field in the multilayered phantom



(a) PIFA and insulator parameters



(b) Feeding and cavity parameters

Fig. 7. Final antenna layout

Figure 8 shows the input reflection coefficient of this antenna in a homogenous muscle phantom, compared to the multilayered phantom. As expected, we see that the homogenous phantom is good enough to design the antenna. However, and due to the effect illustrated in Figure 6, it is very important to use the multilayered phantom to characterize the transmission between the implanted antenna and the wearable antenna on the external node.

TABLE III. DIMENSIONS OF FINAL PIFA. THE ANTENNA IS PLACED IN A CAVITY AND COVERED WITH PEEK. DIMENSIONS IN MM

Material	PIFA_w	feed_pos	sub_h	ins_h	sub_h	cav_w
Free space	3.63	0.51	1.27	0.73	8	10
Muscle (lossless)	3.3	1.24	1.27	0.73	8	10
Muscle (Lossy)	3.3	1.24	1.27	0.73	8	10
Multilayered phantom	3.3	1.24	1.27	0.73	8	10

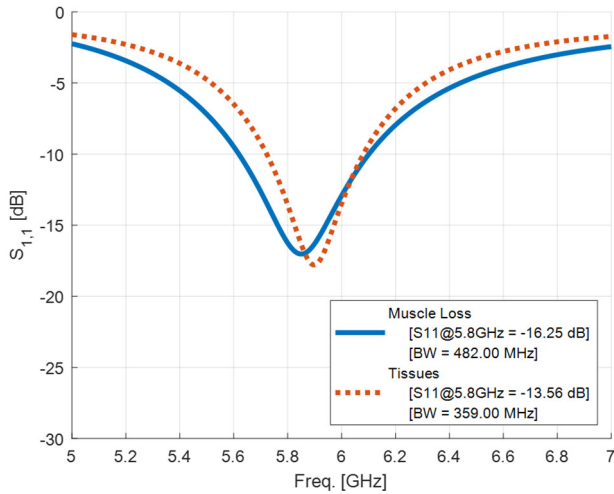


Fig. 8. PIFA S_{11} for the antenna placed in a homogenous lossy muscle phantom and in the multilayered phantom

The wearable node antenna is a simple patch antenna covered by a layer of PEEK that was placed directly on the top of the phantom. The S_{21} between the two nodes is depicted in Figure 9, and shows that the loss is smaller than 25 dB over our frequency band of interest. It is interesting to note that this number coincides well with the simplified model described in Figure 2. Initial measurements performed on a phantom made of animal bone, muscle fat and skin and using a non-optimized version of the antennas confirm these results, and will be shown at the conference along with further measured results. In these preliminary measurements, the attenuation between the two nodes was of 40 dB (the expected value according to simulations for the non optimal antennas was 32 dB).

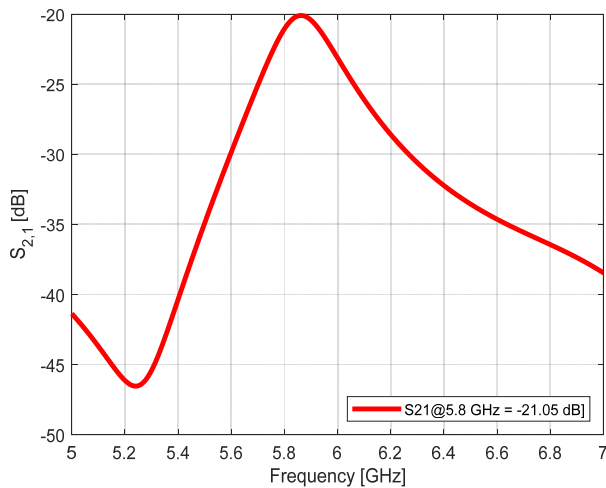


Fig. 9. Transmission coefficient between the implanted and wearable nodes

VI. SUMMARY

We have discussed some possible design strategies to design antennas for body implants, and highlighted some of

numerical and model linked issues that may influence the design process. As an example, an antenna for a cranial implant was designed, and simulation and initial measured are presented. Further measurements will be presented at the conference.

REFERENCES

- [1] C.A. Balanis, *Antenna Theory, Analysis and Design*, Harper and Row, 1982, New York
- [2] M Gustafsson, C. Sohl and G. Kristensson, "Physical limitations on antennas of arbitrary shape", *Proc. R. Soc. A*, vol. 463, pp. 2589-2607, 2007
- [3] A.K. Skrivervik, J.-F. Zürcher, O. Staub and J.R. Mosig, "PCS Antenna Design : The Challenge of Miniaturization", *IEEE AP-Magazine*, Aug. 2001, pp12-27
- [4] C. Ehrenborg and M. Gustafsson, "Calculating physical bounds for in-body antennas", *Proc. the 12th European Conference on Antennas and Propagation, EuCAP 2018*, London, UK, pp 1-3.
- [5] Denys Nikolayev, Maxim Zhadobov, Pavel Karban, and Ronan Sauleau, *PHYSICAL REVIEW APPLIED* 9, 024033 (2018), pp. 024033-1 - 024033-12
- [6] Anja K Skrivervik, Marko Bosiljevac, Zvonimir Sipus, "Fundamental Limits for Implanted Antennas: Maximum Power Density Reaching Free Space", *IEEE Trans. on Antennas and Propagation*, Vol. 68, No8, 2019, pp. 4978 – 4988.
- [7] M. Ackermann, "the visible human project", *Proc. IEEE*, vol. 86, No 3, 1998, pp. 504-511.
- [8] M. Bosiljevac, Z. Sipus, A.K. Skrivervik, "Propagation in Finite Lossy Media: an Application to WBAN", *Antennas and Wireless Propagation Letters, IEEE*, Year: 2015, Volume: 14, PP 1546 – 1549.
- [9] Alberto J. Moreno Montes, "Study of some propagation issues for cranial implants", *Master thesis at the Universidad Carlos III de Madrid*, August 2019.
- [10] N. C. Institute for Applied Physics, 'Dielectric Properties of Body Tissues'. [Online]. Available: <http://niremf.ifac.cnr.it/tissprop/htmlclie/htmlclie.php>. [Accessed: 14-Oct-2019].